Supplementary Information

Transferrin-conjugated drug/dye-co-encapsulated magnetic nanocarriers for active-targeting fluorescent/magnetic resonance imaging and anti-tumor effects in human brain tumor cells

Xueqin Wang*[a], Yanyan Chang [a], Dongxu Zhang [a], Baoming Tian[b], Yan Yang [b] and Fang Wei [b]*

[a] *College of Bioengineering, Henan University of Technology, Zhengzhou, Henan 450001, P.R .China*

[b] *School of Life Sciences, Zhengzhou University, Zhengzhou, Henan 450001,P.R.China*

* *Corresponding authors:* Xueqin Wang, *E-mail address:* wangxq0708@163.com, *College of Bioengineering, Henan University of Technology, Zhengzhou, Henan 450001, P.R .China. Tel.: + 86 371 67756928; fax: + 86 371 67756928.* Fang Wei, *E-mail address:* fangwei@zzu.edu.cn, *School of Life Sciences, Zhengzhou University, Zhengzhou, Henan 450001,P.R.China. Tel.: + 86 371 67739513; fax: + 86 371 67739513.*

This supporting information provides all of the additional information as noted in the manuscript and more detailed discussion of the current study.

Synthesis of SPIO NPs

Superparamagnetic γ-Fe_2O_3nanoparticles(SPIO NPs) used in this study were synthetized from magnetite (Fe_3O_4) according to methods proposed elsewhere.[1, 2] First, 4.5 mL $FeCl_3$ (2 mol/L dissolved in 2 mol/L HCl) was added to 15.5 mL of ultra-

purified water, and then 3 mL Na_2SO_3 (1 mol/L) was subsequently added dropwise into the mixture within 1 min while stirring. When the solution color changed from redto light yellow, the solution was added into 120 mL NH_4OH (0.85 mol/L) while vigorously stirring. A black precipitate quickly formed and was completely crystallized for another 40 min. The black precipitate was washed with deoxygenated water until the solution pH less than 7.5. Then, the precipitate was diluted to concentration 3 mg/ml through the deoxygenated water was added. The solution pH wad adjusted to 3.0 with HCL(0.1 mol/L), and maintained at this pH for 5min. The solution temperature was raised to 90 ℃ rapidly by heating, then vigorously stired 90 min at 110 ℃.The black precipitate became brown, washed it with distilled water and then dried to form SPIO NPs powder.

The magnetically responsive and stability of Tf-CS/SPIO NPs

The magnetic response and stability of prepared Tf-CS/SPIO NPs in different media were analyzed according to the previously described protocol.[3] The Tf-CS/SPIO NPs (100 μg/mL) were ultrasonically dispersed in the De-ionized (DI) water, the RPMI-1640 culture medium, and the phosphate-buffered saline (PBS, pH 7.4) at RT in the magnetic field respectively. The magnetic responsiveness and stability were then examined by measuring the optical absorbance of the tested dispersions at the predetermined time points using a UV-Vis spectrophotometer at 480 nm.

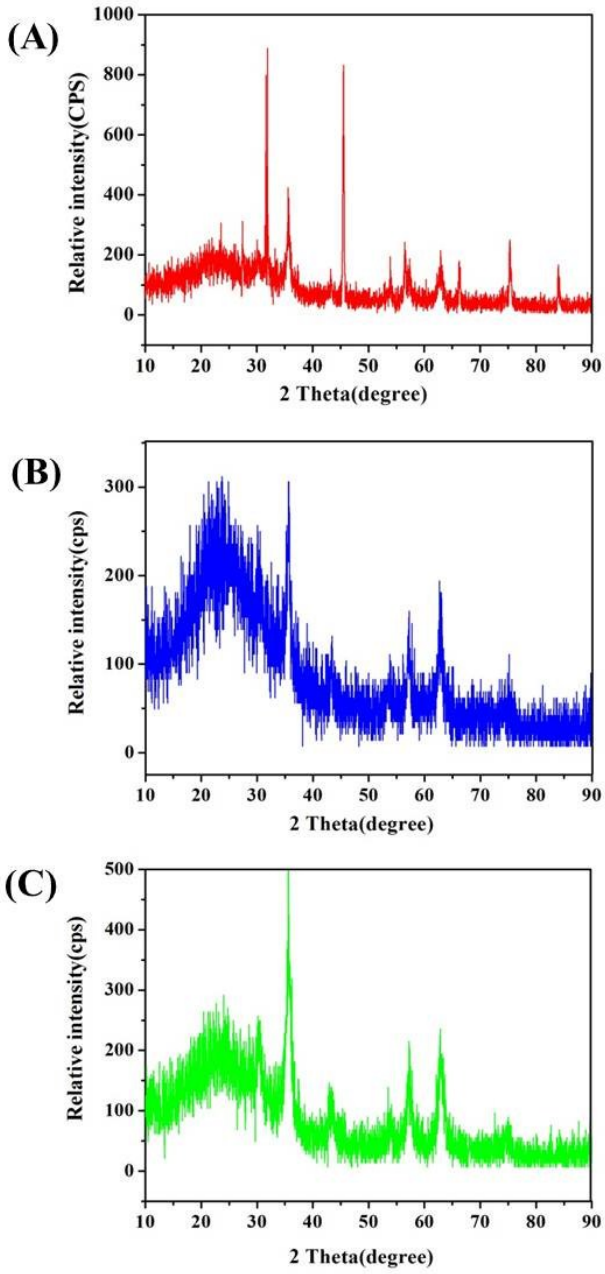

Fig. S1 XRD pattern of SPIO NPs (A), CS/SPIO NPs (B), and Tf-CS/SPIO NPs (C).

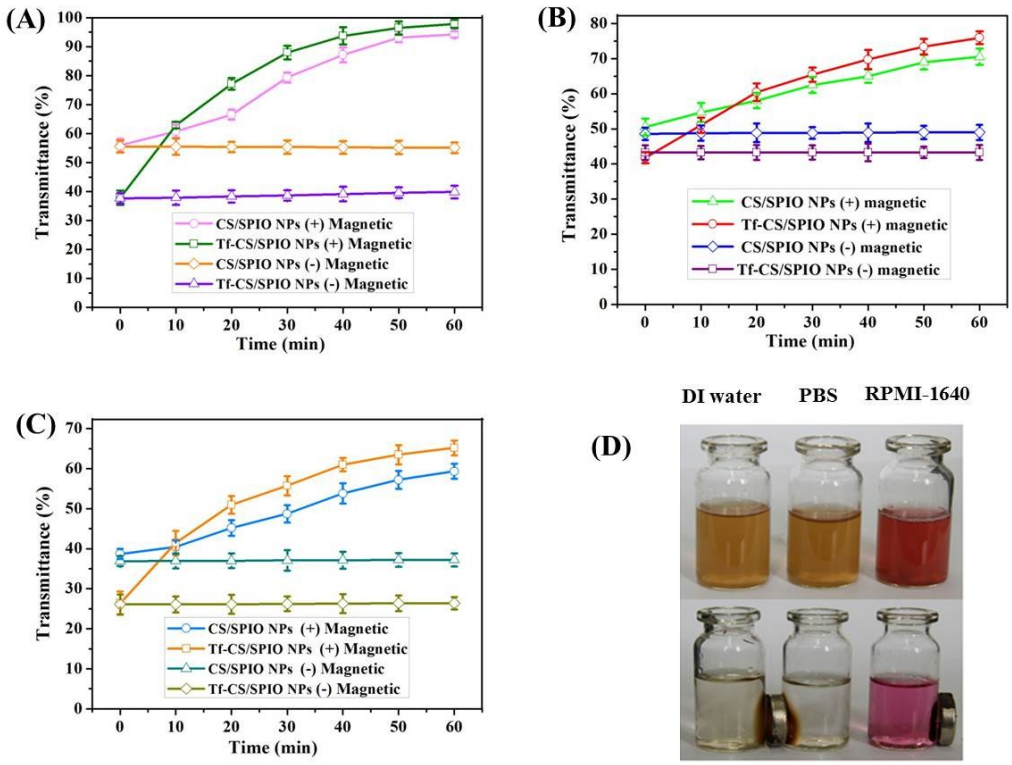

Fig. S2 Magnetic response property and stability of CS/SPIO NPs or Tf-CS/SPIO NPsin DI water (A), PBS solution (pH 7.4) (B), RPMI-1640 culture medium (C) , and their corresponding images by adding and removing an external magnetic field in different medium.

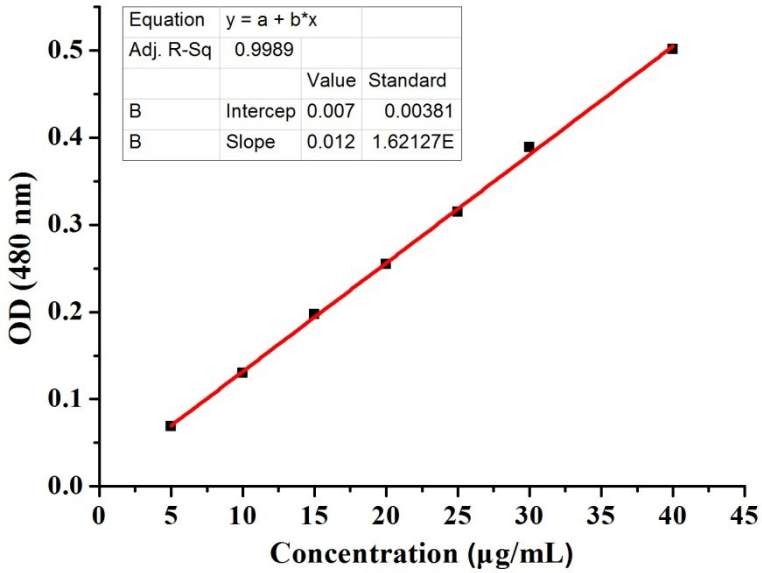

Fig. S3 The calibration curve of DOX content

Actin cytoskeleton

Cytoskeleton microfilaments are commonly involved in normal cell attachment and morphology; thus, the altered appearance of actin in the U251 MG cells suggested that DOX-Tf-CS/SPIO NPs are highly cytotoxic. The staining of actin cytoskeleton using Rhodamine phalloidin could specifically bind with high affinity to the polymerized form of F-actin.[4] Fig. S4 shows the result of immunocytochemistry

staining of the actin cytoskeleton. The results showed that the targeting DOX-Tf-CS/SPIO NP-treated U251 MG cells displayed obvious differences, including reduced cell surface and nuclei and fractured cytoskeleton compared with the CS/SPIO NP- and Tf-CS/SPIO NP-treated U251 MG cells.

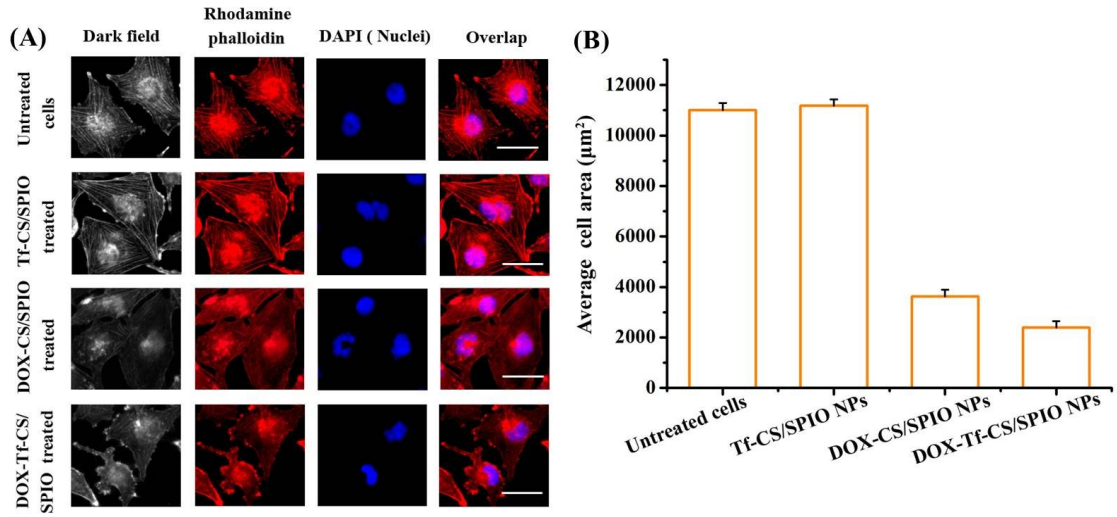

Fig S4. Immunofluorescent staining of actin cytoskeleton of the treated U251 MG cells using the rhodamine phalloidin (red). The treated U251 MG cells with different nanocarriers were cultured for 24 h. Cells were located by counterstaining with DAPI (blue). Untreated U251 MG cells were used as blank controls. Scale bar = 50 μm.

Intracellular ROS and calcium handling

ROS-induced oxidative stress is one of the crucial factors responsible for NP cytotoxicity.[5, 6] Intrinsic antioxidant defense system protects the body against ROS by keeping a balance between the oxidant/antioxidant levels in cells. However, excessive ROS generation resulting from impaired antioxidant defense system of the body induces oxidative stress, resulting in DNA damage, mitochondrial dysfunction, and apoptotic cell death.[7] ROS levels during NP treatment was investigated via DCFH-

DA assay using an inverted fluorescence microscope equipped with a high-resolution CCD camera to assess the potential role of ROS in oxidative stress-mediated cell death. DCFH-DA is a membrane-permeable dye used to measure intracellular ROS activity. Within the cells, DCFH-DA is cleaved by intracellular esterases and finally converted into highly fluorescent DCF in the presence of ROS.[8] The level of ROS generation in DOX-CS/SPIO NP- and DOX-Tf-CS/SPIO NP-treated U251 MG cells obviously increased compared with that of untreated and Tf-CS/SPIO NP-treated U251 MG cells (SI, Fig. S5). Moreover, DOX-Tf-CS/SPIO NPs induced more oxidative stress in U251 MG cells compared with DOX-CS/SPIO NPs resulting from the Tf-mediated targeted delivery of DOX that induces increased ROS generation. Cytoplasmic Ca^{2+}, which acts as a second messenger, widely regulates various cellular, physiological, and biochemical activities.[59] Fig. S6 shows that no difference exists between the untreated cells and the Tf-CS/SPIO NP-treated U251 MG cells in terms of surface plot graphs and fluorescence intensity. However, the fluorescence intensity of the DOX-Tf-CS/SPIO NP-treated U251 MG cells was obviously enhanced, indicating a robust increase in intracellular Ca^{2+} concentration in treated cells.

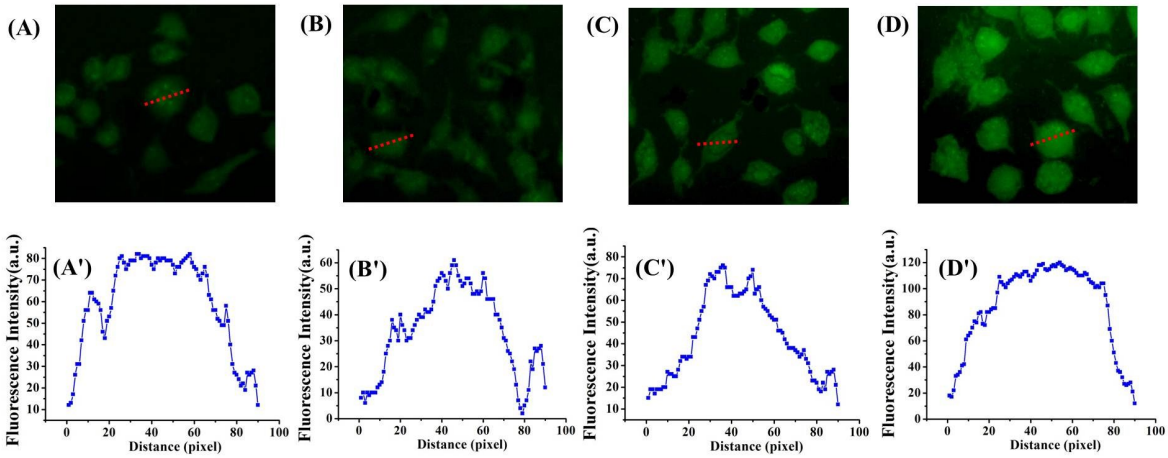

Fig. S5 Analyses of ROS production in U251 MG cells treated with DOX-Tf-CS/SPIO NPs.

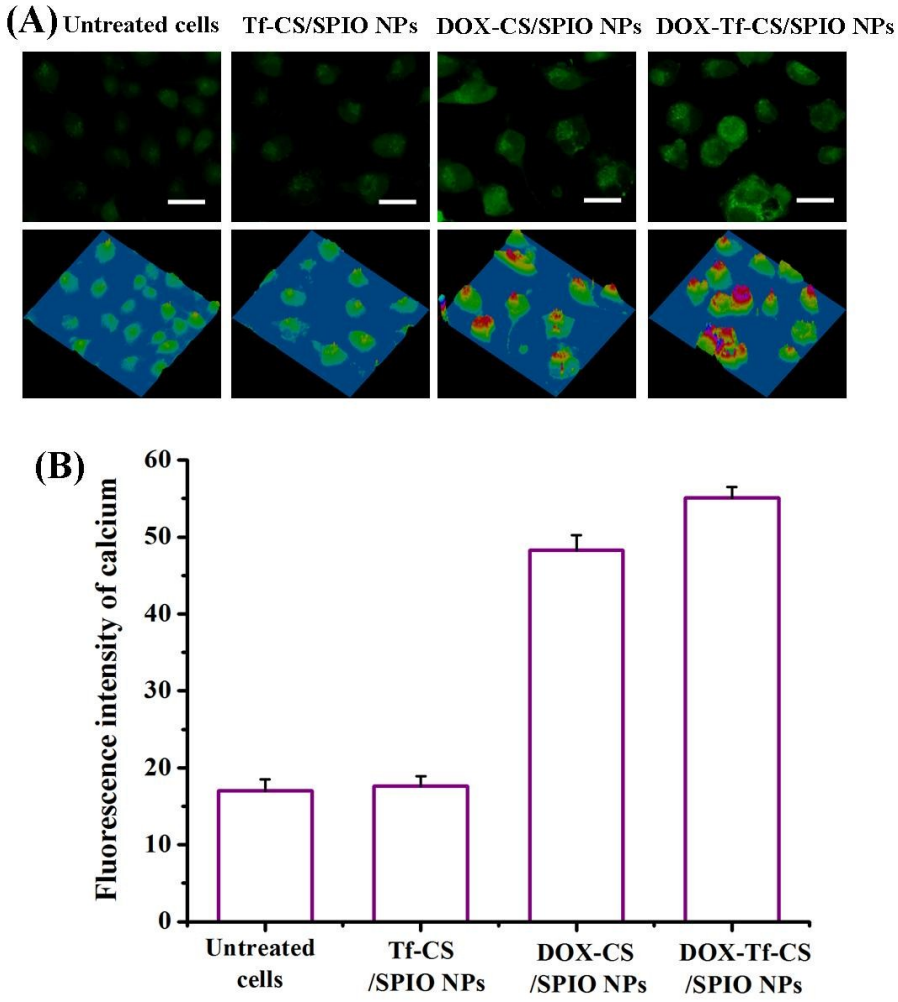

Fig. S6 (A) Fluorescent micrographs of Calcium handling of the untreated and treated U251 cells. (B) The surface fluorescence intensity graphsand analysis of fluorescence intensity. The fluorescence analysis was analyzed using Image-Pro Plus 6.0 software. Scale bar = 50 μm.

References

1 S. Qu, H. Yang, D. Ren, S. Kan, G. Zou, D. Li and M. Li, Magnetite nanoparticles prepared by precipitation from partially reduced ferric chloride aqueous solutions,*J* .*Colloid Interface Sci.*, 1999, **215**, 190-192.

2 Y.K. Sun, M. Ma, Y. Zhang and N. Gu, Synthesis of nanometer-size maghemite particles from magnetite, *Colloids Surf. A. Physicochem Eng Aspects*, 2004*,* **245**, 15-19.

3 X. Wang, L. Wang, X. Tan, H. Zhang and G. Sun, Construction of doxorubicin-loading magnetic nanocarriers for assaying apoptosis of glioblastoma cells, *J. Colloid Interface Sci.*, 2014, **436C**, 267-275.

4 J.Y. Ye, E.Y. Liang, Y.S. Cheng, G.C. Chan, Y. Ding, F. Meng, M.H. Ng, B.H. Chong, Q. Lian and M. Yang, Serotonin enhances megakaryopoiesis and proplatelet formation via p-Erk1/2 and F-actin reorganization, *Stem Cells*, 2014, **32**, 2973-2982.

5 E. Jäger, A. Höcherl, O. Janoušková, A. Jäger, M. Hrubý, R. Konefał, M. Netopilik, J. Pánek, M. Šlouf, K. Ulbrich and P. Štěpánek, Fluorescent boronate-based polymer

nanoparticles with reactive oxygen species (ROS)-triggered cargo release for drug-delivery applications. *Nanoscale*, 2016, **8**, 6958-6963.

6 M. Hanot-Roy, E. Tubeuf, A. Guilbert, A. Bado-Nilles, P. Vigneron, B. Trouiller, A. Braun and G. Lacroix, Oxidative stress pathways involved in cytotoxicity and genotoxicity of titanium dioxide (TiO_2) nanoparticles on cells constitutive of alveolo-capillary barrier in vitro, *Toxicol in Vitro*, 2016, **33**, 125-135

7V. Rani, G. Deep, R.K. Singh, K. Palle and U.C. Yadav, Oxidative stress and metabolic disorders: Pathogenesis and therapeutic strategies, *Life Sci.*, 2016, **148,** 183-193.

8 C. Zhang, L. Yang, X.B. Wang, J.S. Wang, Y.D. Geng, C.S. Yang and L.Y. Kong, Calyxin Y induces hydrogen peroxide-dependent autophagy and apoptosis via JNK activation in human non-small cell lung cancer NCI-H460 cells, *Cancer Lett.*, 2013, **340**, 51-62.

9 G. Zhao, T. Li, D.X. Brochet, P.B. Rosenberg and W.J. Lederer, STIM1 enhances SR Ca^{2+} content through binding phospholamban in rat ventricular myocytes,*Proc. Natl. Acad. Sci. USA.*, 2015, **112***,* E4792-E4801.